



**HAL**  
open science

## Optimization of ceramic content in nickel–alumina composite coatings obtained by low pressure cold spraying

M. Winnicki, S. Kozerski, A. Malachowska, Lech Pawlowski, M. Rutkowska-Gorczyca

### ► To cite this version:

M. Winnicki, S. Kozerski, A. Malachowska, Lech Pawlowski, M. Rutkowska-Gorczyca. Optimization of ceramic content in nickel–alumina composite coatings obtained by low pressure cold spraying. *Surface and Coatings Technology*, 2021, 405, pp.126732. 10.1016/j.surfcoat.2020.126732 . hal-03281839

**HAL Id: hal-03281839**

**<https://unilim.hal.science/hal-03281839>**

Submitted on 15 Dec 2022

**HAL** is a multi-disciplinary open access archive for the deposit and dissemination of scientific research documents, whether they are published or not. The documents may come from teaching and research institutions in France or abroad, or from public or private research centers.

L'archive ouverte pluridisciplinaire **HAL**, est destinée au dépôt et à la diffusion de documents scientifiques de niveau recherche, publiés ou non, émanant des établissements d'enseignement et de recherche français ou étrangers, des laboratoires publics ou privés.



Distributed under a Creative Commons Attribution - NonCommercial 4.0 International License

## Optimization of ceramic content in nickel –alumina composite coatings obtained by low pressure cold spraying

M. Winnicki<sup>1)</sup>, S. Kozerski<sup>1)</sup>, A. Małachowska<sup>1)</sup>, L. Pawłowski<sup>2)1)</sup>, M. Rutkowska-Gorczyca<sup>1)</sup>

<sup>1)</sup> Faculty of Mechanical Engineering, Wrocław University of Science and Technology, Łukasiewicza 5, 50-371 Wrocław, Poland

<sup>2)</sup> IRCER UMR CNRS 7315, University of Limoges, 87068, Limoges, France

### Abstract

The paper describes the technology of nickel-alumina composite coatings obtained by low-pressure cold spray (LPCS). The content of alumina reinforcement was optimized by mixing the commercial K32, being a mechanical mixture of  $\text{Al}_2\text{O}_3 + 50 \text{ wt. \% Ni}$ , with the Ni-cladded alumina powders developed in present study. The cladded powders were prepared by hydrogen reduction method. Two powders including Ni-films covering  $\text{Al}_2\text{O}_3$  particles were developed:  $\text{Al}_2\text{O}_3 + 70 \text{ wt. \% Ni}$  (powder #1) and  $\text{Al}_2\text{O}_3 + 80 \text{ wt. \% Ni}$  (powder # 2). The morphology of obtained cladded powders, analyzed using scanning electron microscope (SEM), showed a porous, cauliflower-like morphology in cladded layer of powder # 1 and dense nickel layer in powder # 2. The measurements of granulometry enabled finding the powder size distribution of pure alumina powder having a mean value of about  $50 \mu\text{m}$  which increased by cladding to about  $70 \mu\text{m}$  in powder # 1 and to about  $65 \mu\text{m}$  in powder # 2. The cladded powders were mixed with K32 powder and sprayed using LCPS onto mild steel substrate. The microstructure of obtained coatings was characterized using SEM, energy dispersive X-ray spectroscopy (EDXS) and electron backscatter diffraction (EBSD). The graphical analysis of coatings' cross-sections enabled determining content of alumina in sprayed deposits. This content increased from about 7 % in K32 powder sprayed coatings to 9 – 13 % in coatings obtained using its mixtures with powder # 2 and up to 20 – 30 % for mixtures with powder # 1. The microhardness of coatings sprayed using the mixtures of powder # 1 with powder K32 as well as the coating sprayed only with the powder K32 were slightly greater than  $\text{HV } 0.1 > 150$ . The microhardnesses of about  $\text{HV } 0.1 \approx 200$  was reached for the coatings sprayed using mixtures of powder # 2 with K32. Finally, the bond strength of the sprayed coatings, measured using test ISO 14916, was in the range from 1.7 to 5.9 MPa. The greatest bond strength was reached for the coatings sprayed using powder K32.

### Keywords

Low-pressure cold spray, nickel-alumina composite, metal matrix composite, nickel cladded alumina powder, cermet coatings

---

<sup>1</sup> Corresponding authors, E-mail : [pawlowski.lech@gmail.com](mailto:pawlowski.lech@gmail.com) phone: and +(33) 630 12 32 45

## 1. Introduction

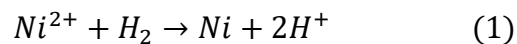
The manufacturing of hydrogen and of its mixture with methane and carbon oxides known as *syngas* (synthetic gas) is an important chemical process of treatment the natural gas. Hydrogen, being the major product of this synthesis, is in consideration to become a major source of energy in the future [1, 2]. The reactions, leading to this synthesis, concern transformation of methane or methanol with the use of *dry reforming* with  $\text{CO}_2$  and *steam reforming* using  $\text{H}_2\text{O}$  at high temperature. The reactions are realized in presence of catalysts being noble metals as e.g. Rh or Pd and non-noble metals as Ni, Co, Cu onto inert supports such as e.g.  $\text{ZnO}$ ,  $\text{Al}_2\text{O}_3$  or  $\text{MgO}$  [1, 3]. A nickel-based catalysts activity are affected by the reduction degree of nickel species and the interaction between metal and support [4]. The low cost of such catalysts is one of important reasons of their application in the *steam reforming* processes [5, 6]. A particular attention has been paid on the nickel catalyst onto alumina support. The latter is probably most frequently used in catalyzers due to its high specific surface area, which provides a high dispersion of the metallic phase [6]. A preparation method plays an important role in affecting the metal-support interactions of the nickel-alumina catalyst and thus deactivation can be omitted [4]. Bang et al. [7] fabricated an ordered mesoporous nickel-alumina catalyst with a structure modifier (trimethylbenzene) and as a result obtained the enhanced mesoporous structure with small metallic nickel. Yoo et al. [8] prepared nickel-alumina catalysts using various compositions of butyric acid assisted nickel precursor solution. The catalysts with the highest nickel dispersion exhibited the best catalytic efficiency in the steam reforming of natural gas. The authors, as Seo *et al.* [9] prepared the mesoporous  $\text{Ni-Al}_2\text{O}_3$  composites by different methods and analyzed their catalytic performances. Yenumala et al. [10] activated the reaction of hydro-deoxygenation of *karanja* oil using similar composite.

The films and coatings deposition technologies can be useful to preparation of metal-oxide composites.  $\text{Ni-Al}_2\text{O}_3$  composite coating was obtained by the use of electroplating by Bahrololoom and Sani [11]. Thermal spraying technologies are also frequently used to obtain such composites. Grewal et al. [12] applied high-velocity oxy-fuel (HVOF) to spray nickel-alumina coatings to be applied against wear. However, high temperature of flame involved in the process resulting in melting of metallic phase at spraying, may deteriorate the functionality of coating by modification of microstructure or, by high temperature oxidation [13]. Therefore, low-temperature processes, such as cold spray, are of great interest. In the spray process, powder particles are accelerated by working gas in the de Laval nozzle to reach supersonic velocities enabling to build up a coating without particles' melting. The particles velocities have to greater than critical one. Such velocity leads to the plastic deformation of particles impacting the substrate enabling their bonding [14, 15].

Irissou *et al* [16] as well as Li *et al.* [17] used cold gas spraying to deposit, respectively, Al and Ni composites with  $\text{Al}_2\text{O}_3$ . The applied techniques used high - [18] and, much less expensive, low-pressure cold spraying (LPCS), which was used by authors of study [19] and in the present study. The metal matrix composite (MMC) coatings can be sprayed using mechanical mixture of metal and oxide powders. However, the cohesion of metal to ceramic grains inside coating is not very high [19]. To improve it, and to increase the content of ceramics in MMC deposit, the ceramic powder particles can be cladded with thin metal layer. This technology was initiated by the authors of [18] and is tested in the present study.

The cladding may enable to distribute more homogeneously ceramic in the sprayed coating and to increase the retention of ceramics in MMC coatings. The issue was analyzed by numerical simulation by Chakrabarty and Song [19]. The authors recommended thermal softening of metallic substrate.

The methods of coated powders manufacturing include mainly [20]: (i) immersion coating; (ii) electroless chemical plating; (iii) electrolytic deposition; (iv) mechanical coating; (v) chemical vapor deposition; and, (vi) physical vapor deposition. Another technique developed and patented in the company *Sherritt Gordon Mines*, bases onto hydrogen reduction of metal salt in an ammoniated solution at high temperature and high pressure [21]. In this method the metal, such as Ni, cations precipitates onto oxide particles and the reduction occurs following the reaction [22]:



This method was applied in the present paper to coat alumina particles with nickel.

## 2. Experimental

### 2.1. Powder fabrication technology

The nickel-alumina cladded powders, were prepared by nickel-hydrogen reduction method in the autoclave. Ammonium sulfate, nickel sulfate hexahydrate and ammonia were used in the synthesis as starting materials. The starting products were prepared as aqueous solution with  $pH \approx 8$ . Alumina powder (KOS, Koło, Poland) was poured in the autoclave and activated with palladium chloride and anthraquinone. The cladding process was carried out under hydrogen pressure of 3 MPa at chamber temperature of 453 K. Two type of powders were developed: (i) powder # 1 of  $Al_2O_3 + 70$  wt. % Ni; and, (ii) powder # 2 of  $Al_2O_3 + 80$  wt. % Ni. The commercial powder used in the cold spray experiments was K32 (Centre for Powder Spraying, Obninsk, Russia). The latter is a mixture of  $Al_2O_3 + 50$  wt. % Ni in which nickel is dendritic and has irregular shape and the particles have size of  $-45+15 \mu m$ .

The preliminary experiments revealed that the cladded powders sprayed separately did not enable obtaining coatings. Consequently, their mixtures with commercial of K32 powder were prepared. The chemical compositions of the mixtures are presented in Table 1.

### 2.2. Spray process

The powders were sprayed onto steel *S235JR* substrate having size 3x25x50 mm using low-pressure cold spray device, *Dymet 413* (Centre for Powder Spraying, Obninsk, Russia). The substrates were initially degreased and grit-blasted with alumina powder having size about  $850 \mu m$  prior to spraying. The cold spraying gun was equipped in an internal gas heater and *de Laval* nozzle with an outlet diameter of 5 mm. The gun was attached to xy-moving set-up made by *BZT Maschinenbau* (Leopoldshöhe, Germany). The traverse speed of 5 mm/s was used in the experiments. The powders were injected to the torch radially in the beginning of divergent part of the nozzle. Stand-off distance between nozzle exit and substrate surface was about 10 mm and the distance between neighboring spraying paths was 2 mm.

The initial tests carried out using cladded powder # 1 did not allow to reach adhesion to the substrate at any LPCS parameters used. The further tests were carried out with the feedstock with powder # 2. Moreover, the optimization included the additional substrate heating at deposition and the use of nitrogen as the working gas. The build-up of coatings started while substrate was heated up to 773 K and nitrogen was used as working gaz. Finally, it was decide to use the mixtures of cladded powders with commercial powder K 32 sprayed using air was used as a working gas under the pressure of 0.9 MPa and at temperature of 873 K. All the samples were sprayed with the same parameters including powder feeder setting and torch kinetics. The time of coatings deposition was constant equal to about 1.5 min.

### 2.3. Powders and coatings characterization

The morphology of nickel-alumina powders as well as surface and microstructure of deposited coatings were analyzed using SEM type Zeiss *Leo 1455VP* (Zeiss, Jena, Germany) microscope equipped with secondary electrons (SE) and back-scattered electrons (BSE) detectors. The electron backscattered diffraction (EBSD) analysis was carried out using Zeiss *Supra 35* scanning electron microscope equipped in energy dispersive X-ray spectroscopy (EDXS) Trident XM4 system with 15 kV accelerating voltage and 17 mm working distance. The powders particles' sizes were determined with the use of set-up *Cilas 930* (Cilas, Orléans, France). The specimens for metallographic investigations were prepared by cutting of the coated samples and embedding in epoxy resin. The surfaces of the cross-sections were polished, and finished with suspension having diamond particles sizes of 1  $\mu\text{m}$ . The semi-quantitative graphic analysis using *ImageJ* version 1.50i free-accessible software enabled checking out the quantity of alumina particles in the deposited coatings. The analyses were made on three coatings cross-sections corresponding to each composition of sprayed powders (see Table 1).

The Vickers microhardness of sprayed coatings was measured using tester *MMT-X7 Matsuzawa C* (Akita, Japan) using a load of 0.98 N. At least 10 indentations were made in each coating cross-section to have the mean HV0.1 value. The coatings' adhesion to the substrate was estimated using tensile pull-off test described in the ISO 14916:2017-05 standard. An *Elcometer 510-20T* (Manchester, England) device was used. Three tests were carried out for a coating sprayed with each powder compostion to find a mean adhesion.

## 3. Results and discussion

### 3.1. Powder manufacturing

Alumina powder used for cladding have particles with irregular shape and an average size of about 40  $\mu\text{m}$  (see Fig. 1). The manufactured powders were prepared by cladding of Ni layer on the alumina particles. Two cladded powders were manufactured:

- powder # 1 including  $\text{Al}_2\text{O}_3$ +70 wt. % of Ni with mean diameter slightly greater than 70  $\mu\text{m}$  and ceramic particles covered with thin metallic layer being relatively porous and having cauliflower-like microstructure shown in Fig. 2;
- powder # 2 including  $\text{Al}_2\text{O}_3$ +80 wt. % of Ni with mean diameter close to 65  $\mu\text{m}$  and ceramic particles covered with relatively thick, dense and regular metallic layer shown in Fig. 3.

The nickel clad on  $\text{Al}_2\text{O}_3$  particles in powder # 1 seems to be continuous after the hydrogen reduction process as shows it Fig. 2. The clad has cauliflower-like microstructure and some porosity inside cladded layer is visible. Li [17] observed similar cauliflower microstructure of cladded Ni layers onto alumina particles. Such cauliflower-like and porous microstructure seems to occur at small thicknesses of metallic layer. The microstructure becomes denser with increasing thickness resulting from longer time of cladding. Such morphology has Ni clad on particles of powder # 2 shown in Fig. 3. However, the distribution of particles sizes of this powder has a maximum at about 65  $\mu\text{m}$  being slightly smaller than that in powder # 1. The difference could have resulted from the different microstructure of cladded layer, which became denser and smoother. The commercial K32 powder being a mixture of  $\text{Al}_2\text{O}_3$  and Ni is shown in Fig. 4. The dendritic morphology of nickel particles is important. The previous experience of LCPS deposition of Ni made in our laboratory revealed that the coatings do not build-up while using spherical particles. On the contrary, the use of dendritic-shape ones enabled LPCS coatings to be obtained.

### 3.2. Microstructure of coatings

The microstructures of coatings cold sprayed with commercial K32 powder and with the powder mixtures including manufactured cladded powders are shown in Fig. 5 and Fig. 6. The coating showing the densest microstructure was sprayed using commercial powder K32 (Fig. 5a). The coatings were uniform without any defects, such as micro-cracks or large pores. The mixtures of powder K32 with cladded powders enabled obtaining coatings having different microstructures. The latter depended mainly on the quantity of K32 powder in the mixture and on the thickness of nickel clad of powder used in the mixture. The increase of nickel content in sprayed powder resulted in coatings being denser and having greater thickness (shown in Table 2). The coatings deposited with mixtures including powder # 1, being cladded with thin nickel layer, had many longitudinal micro-cracks visible in Figs 5b-d). The coatings deposited with mixtures of powder # 2 were much denser. These powder particles must have adhered better to the substrate and previously deposited coating at processing forming deposits with less microstructural defects as e.g. coatings P2-75 shown in Fig. 6 a. However, the thicknesses were limited to only 100  $\mu\text{m}$ , and some microcracks are visible. An increase of coating's thickness and of their quality followed the increase of K32 powder in powders mixtures. Consequently, the coatings sprayed using powders mixtures P1-33 and P2-33 had dense microstructure and greatest thickness as shows it Fig. 5f and Fig. 6d. The microstructure of theses coatings had less defects than that of the ones sprayed using mixtures P1-50 and P2-50. These coatings had some local porosity and micro-cracks visible under greater magnification in Fig. 7. It should be also noted that surface of the coating's was much rougher in the case of coatings deposited using powder # 1 mixtures. This may have resulted from cauliflower-like microstructure of Ni-clad in the powder # 1. Similar observation concerning the optimal content of metal in cold sprayed powders mixtures of aluminum with alumina was observed by Irrisou *et al.* [16]. These authors found out that the maximum content of alumina in cermet could not be exceed 25 wt. %.

The microstructure of optimized coating obtained with the mixture P1-33 was analyzed more carefully. The micrograph of cross-section at higher magnification shown in Fig. 8 enables visualizing why spraying of powder # 1 did not allow to build-up a coating. The nickel clad covering alumina particle was too thin to bond individual cladded particles.

Consequently, mixing with powder K32, being rich in nickel, was necessary. Moreover, Fig. 8 shows that the impact of cladded alumina particles on the substrate (or previously deposited coating) resulted in cracking inside alumina core. Subsequently, it is reasonable to deduce that many small alumina particles could have been at impact. The presence of small  $\text{Al}_2\text{O}_3$  particles is confirmed by the mapping of Al and of Ni made on the cross-section of coatings sprayed using mixtures P1-33 and P2-33 in Figs 9 and 10.

EBSD analyses were carried out to examine the preferred crystallographic orientations of nickel grains in the region rich in alumina (about 69 %). The transformation map and the polar figures indicated that nickel particles did not have preferred crystallographic orientation. Such orientation did not occur neither in the close neighborhood of alumina particles. The analysis enable concluding, that high kinetic energy of sprayed particles process could have resulted in plastic deformation and in generation of heat.

The application of the mixture of nickel cladded alumina with commercial powder K32 aimed at increasing the limit of alumina content in the sprayed deposits. The graphical analysis of sprayed coatings cross-section enabled estimating the content of alumina in the deposits shown in Table 2. The coatings sprayed with K32 powder included 7.3 % of  $\text{Al}_2\text{O}_3$ . The coatings sprayed using the mixtures showed increase in alumina volume. The greatest values of 30.5% and of 12.7% of alumina were reached for the coatings sprayed using the powder mixtures P1-70 and P2-67. The powder mixtures prepared with powder # 1 enabled obtaining coatings with higher ceramic content than that obtained with powder # 2 mixtures. Moreover, the alumina content in coatings is the greatest for the mixtures including about 70 % of cladded powders. Consequently, it seems that the use of more than 30% of commercial K32 powder in the powder mixtures led to increase of nickel content in the coatings. It can be explained by the adherence of nickel particles to the substrate (or previously deposited coating) and by their participation in the coating build-up. On the contrary, hard ceramic particles may easily rebound after impact.

### 3.3. Mechanical properties of coatings

The results of microhardness measurements of LCPS sprayed coatings are presented in Fig. 11. The coatings sprayed with the use of powder # 2 mixtures showed significantly higher hardness comparing to that sprayed with powder # 1 mixtures and to that obtained with pure K32 powder. The highest and the lowest mean values of HV0.1 for powder # 2 sprayed coatings are about 220 (powder P2-67) and 190 (initial powder P2-33) comparing with 167 obtained for coating sprayed using K32 powder. Thick Ni-clad on the alumina particles occurring in powder # 2 particle could have better protected ceramic cores against crushing and rebounding. The microhardnesses of coatings cold with mixtures including of powder # 1 mixtures are the lowest ones. The low microhardness values correlate well with the coatings microstructure, which shows many cracks and porosity (see Fig. 5 and Fig. 8).

The bond strengths of tested cermet coatings are presented in Fig. 12. The used ISO 14916:2017-05 standard requires that the coatings should have sufficient thickness to prevent glue penetration through the coating porosity towards the substrate. Consequently, the pull-off tests were performed only for the coatings being thicker than 100  $\mu\text{m}$ , i.e. sprayed with the powder K32 and the mixtures P1-50, P1-33, P2-50, P2-33. The greatest

bond strength of 5.9 MPa had the coating deposited using commercial K32 powder. The coatings sprayed using all the mixtures of powders had smaller bond strength. This can be explained by the effect of high ceramic content in which lowered coatings' adhesion. The failures observed at bond strength tests were as follows: (i) adhesive (sample P1-33); (ii) adhesive-cohesive (sample P1-50); and (iii) cohesive-epoxy-resin (sample P2-33, P2-50 and K32).

## Conclusion

The study aimed at developing cermet coatings with alumina and nickel with possibly large scale of ceramic content to be used with cheap low pressure cold spray technology. The usual technology consists of spraying the mechanical mixture of ceramic with metal powders. This technology was modified by adding the cladded powders. The powders were developed in present study included alumina particles covered by a nickel layer. The cladding was realized by hydrogen reduction method to reach two compositions, namely: (i)  $\text{Al}_2\text{O}_3$  + 70 wt. % Ni being called powder # 1; and, (ii)  $\text{Al}_2\text{O}_3$  + 80 wt. % Ni being powder # 2. The morphology of powder # 1 Ni-cladding was porous and cauliflower-like. Powder # 2 had Ni-layer thick and relatively dense. The granulometries measurements enabled finding the mean size of cladded powders to be about 70  $\mu\text{m}$  in powder # 1 and 65  $\mu\text{m}$  in powder # 2. The cladded powders were mixed in a few proportions with a commercial K32 powder being a mixture of  $\text{Al}_2\text{O}_3$  + 50 wt. % Ni. The final mixtures were sprayed onto mild steel substrate. The microstructure characterizations of obtained coatings characterized using SEM, EDXS and EBSD enabled to find that the densest deposits were obtained while spraying commercial powder and its mixtures with about 33 wt. % of both cladded powders. The content of alumina particles in sprayed deposits increases by application of mixtures from about 7 % of for K32 powder sprayed coatings to 9 – 13 % in coatings obtained its powder # 2 mixtures , up to 20 – 30 % for coatings sprayed with powder # 1 mixtures. The microhardness of coatings including more alumina was surprisingly less hard than the coatings having more nickel. This effect was explained by more intensive crushing of alumina particles at impact with substrate. The bond strength of the sprayed coatings was in the range from 1.7 to 5.9 MPa. The smallest values were reached for the coatings sprayed mixtures using of powder # 1 and the greatest one was reached in coatings sprayed with pure K32 powder. The further studies will be carried out to apply the optimized cermet coatings for catalytic applications.

## References

1. J.L. Contreras , J. Salmenes, J.A. Colin-Luna, L. Nuno, B. Quintana, I. Cordova, B. Zeifert, C. Tapia, and G.A. Fuentes, Catalysts for  $\text{H}_2$  production using the ethanol steam reforming (a review), *Int. J. Hydrogen Energy*, 39 (2014) 18835-53.
2. A. Abdulrasheeda,, A. A. Jalila, Y. Gamboa, M. Ibrahima, H. U. Hambalia, and M.Y. Shahul Hamida, A review on catalyst development for dry reforming of methane to syngas: Recent advances, *Renewable and Sustainable Energy Reviews* 108 (2019) 175–93.
3. S. Sá, H. Silva, L. Brandão, J. M.. Sousa, and A. Mendes, Catalysts for methanol steam reforming—A review, *Applied Catalysis B: Environmental* 99 (2010) 43–57.

4. L. Li, Z. Shang, Z. Xiao, L. Wang, X. Liang, and G. Liu, Steam reforming of n-dodecane over mesoporous alumina supported nickel catalysts: Effects of metal-support interaction on nickel catalysts, *Int. J. Hydrogen Energ.* 44 (2019) 6965-77.
5. S. Ali, M.J. Al-Marri, A.G. Abdelmoneim, A. Jumar, and M.M. Khader, Catalytic evaluation of nickel nanoparticles in methane steam reforming. *Int. J. Hydrogen Energ.* 41 (2016) 22876-85.
6. J. P. da S.Q. Menezes, A. P. dos S. Dias, M. A.P. da Silva, and M. M.V.M. Souza, Effect of alkaline earth oxides on nickel catalysts supported over  $\gamma$ -alumina for butanol steam reforming: Coke formation and deactivation process, *Int. J. Hydrogen Energ.* 45 (2020) 22906-20.
7. Y. Bang, S. J. Han, J. Yoo, J. H. Choi, K. H. Kang, J. H. Song, J. G. Seo, J. Ch. Jung, and I. K. Song, Hydrogen production by steam reforming of liquefied natural gas (LNG) over trimethylbenzene-assisted ordered mesoporous nickel–alumina catalyst, *Int. J. Hydrogen Energ.* 38 (2013) 8751-8.
8. J. Yoo, S. Park, J. H. Song, S. Yoo, and I. K. Song, Hydrogen production by steam reforming of natural gas over butyric acid-assisted nickel/alumina catalyst, *Int. J. Hydrogen Energ.* 42 (2017) 28377-85.
9. J. G. Seo, M. H. Youn, S. Park, D. R. Park, J. C. Jung, J. S. Chung, and I. K. Song, Hydrogen production by steam reforming of liquefied natural gas (LNG) over mesoporous nickel–alumina composite catalyst prepared by an anionic surfactant-templating method, *Catalysis Today* 146 (2009) 44–9.
10. S. R. Yenumala, P. Kumar, S. K. Maity, and D. Shee, Hydro-deoxygenation of *karanja* oil using ordered mesoporous nickel alumina composite catalysts, *Catalysis Today*, in press, <https://doi.org/10.1016/j.cattod.2019.08.040>.
11. M.E. Bahrololoom and R. Sani, The influence of pulse plating parameters on the hardness and wear resistance of nickel–alumina composite coatings, *Surf. Coat. Technol.* 192 (2005) 154– 63.
12. H.S. Grewal, H. Singh, and A. Agrawal, Microstructural and mechanical characterization of thermal sprayed nickel–alumina composite coatings, *Surf. Coat. Technol.* 216 (2013) 78–92.
13. A.S. Jagadeeswar, S. Kumar, B. Venkataraman, and P. S. Babu, A. Jyothirmayi, Effect of thermal energy on the deposition behaviour, wear and corrosion resistance of cold sprayed Ni-WC cermet coatings, *Surf. Coat. Technol.* 399 (2020) 126138.
14. H. Assadi, F. Gärtner, T. Stoltenhoff, and H. Kreye, Bonding mechanism in cold gas spraying, *Acta Materialia* 51 (2003) 4379-94.
15. T. Schmidt, H. Assadi, F. Gärtner, H. Richter, T. Stoltenhoff, H. Kreye, and T. Klassen, From Particle Acceleration to Impact and Bonding in Cold Spraying, *J. Therm. Spray Technol.* 18 (2009) 794-808.
16. E. Irissou, J.-G. Legoux, B. Arsenault, and C. Moreau, Investigation of Al-Al<sub>2</sub>O<sub>3</sub> Cold spray coating formation and properties, *J. Thermal Spray. Technol.* 16 (5-6) (2007) 661-68.
17. W.Y. Li, C. Zhang, H. Liao, J. Li, and C. Coddet, Characterizations of cold-sprayed Nickel–Alumina composite coating with relatively large Nickel-coated Alumina powder, *Surf. Coat. Technol.* 202 (2008) 4855-60.
18. H. Koivuluoto and P. Vuoristo, Effect of powder type and composition on structure and mechanical properties of Cu +Al<sub>2</sub>O<sub>3</sub> coatings prepared by using low-pressure cold spray process, *J. Thermal Spray. Technol.* 19 (5) (2010) 1081-92.

19. R. Chakrabarty and J. Song, Numerical simulations of ceramic deposition and retention in metal-ceramic composite cold spray, *Surf. Coat. Technol.* 385 (2020) 125324
20. S. A. Baban, Production and properties of metal-coated powders for use in the production of engineering components, PhD thesis, Loughborough University, Loughborough, U.K., 1989.
21. V.N. Mackiw, V. Kunda, and, J.B. Haworth, Method of producing composite non-metallic powders, US Patent no 2,853,398, patented 23 September 1958.
22. V. N. Mackiw, W. C. Lin, and W. Kunda, Reduction of nickel by hydrogen from ammoniacal nickel sulfate solutions, *J. Metals*, June (1957) 786-93.

## Figures captions

Fig. 1 Alumina powder used for cladding: a) SEM (SE) of powder's particles cross section; b) particles' sizes distribution.

Fig. 2 Cladded powder # 1 containing  $\text{Al}_2\text{O}_3$  +70 wt. % Ni: a) SEM (BSE) micrograph of powder and of cross sections of the powder particles; b) particles' sizes distribution.

Fig. 3 Cladded powder # 2 containing  $\text{Al}_2\text{O}_3$  + 80 wt. % Ni: a) SEM (SE) micrograph of powder and of cross sections of the powder; b) particles' sizes distribution.

Fig. 4 K32 mixed powder of  $\text{Al}_2\text{O}_3$  + 43 wt. % Ni: a) SEM (BSD) of powder mixture, b) particles' sizes distribution.

Fig. 5. SEM (BSE) micrographs of cross-sections and surfaces of cold sprayed coatings' using powders: a) commercial K32; and mixtures: b) P1-80; c) P1-70; d) P1-60; e) P1-50 and, f) P1-33.

Fig. 6. SEM (BSE) micrographs of cross-sections and surfaces of cold sprayed coatings' using powders mixture: a) P2-75; b) P2-67; c) P2-50 and, d) P2-33.

Fig. 7. SEM (SE) micrographs of cross-sections and surfaces of cold sprayed coatings' using powders: a) mixture P1-50; and, b) mixture P2-50.

Fig. 8. SEM (SE) micrographs of cross-section of coating sprayed using P1-33 mixture showing individual nickel-clad alumina particle.

Fig. 9. SEM micrograph and EDXS map of cross-section of the region rich in alumina of coating sprayed using P1-33 mixture: a) SEM micrograph of region; b) Al map; and, c) Ni map.

Fig. 10 SEM micrograph and EDXS map of cross-section of the region rich in alumina of coating sprayed using P2-33 mixture: a) SEM micrograph of region; b) Al map; and, c) Ni map.

Fig. 11 Microhardness of coatings cold sprayed using powder mixtures. The numbers above the symbols correspond to the mean values.

Fig. 12 Bond strength of coatings cold sprayed using some powder mixtures. The numbers above the symbols correspond to the mean values.

# Figures

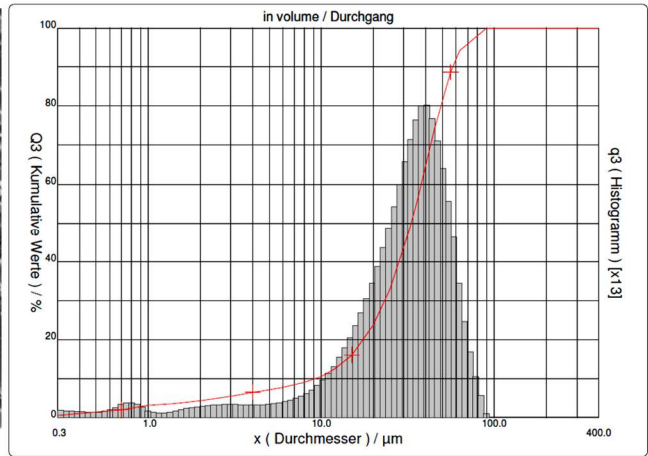
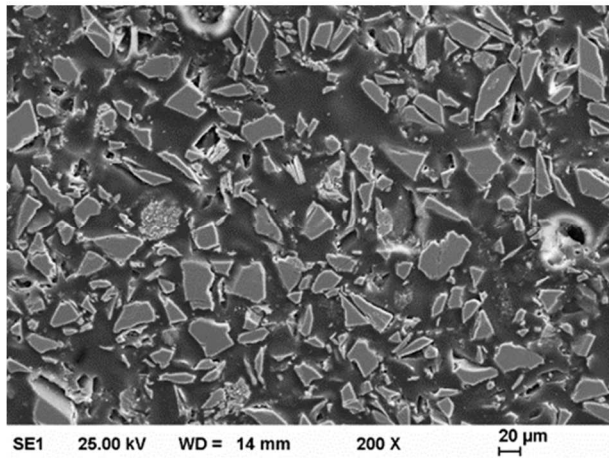


Fig. 1

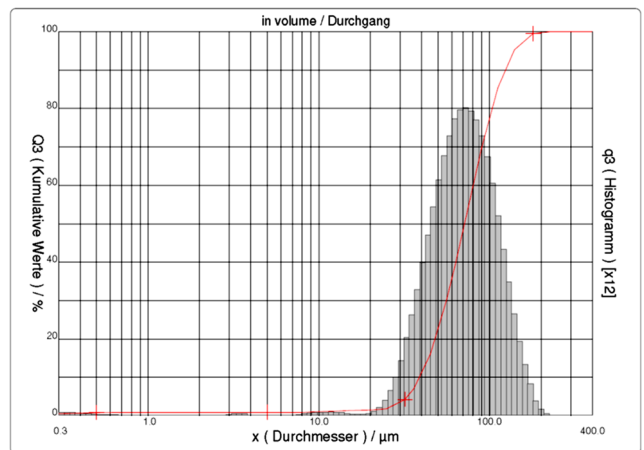
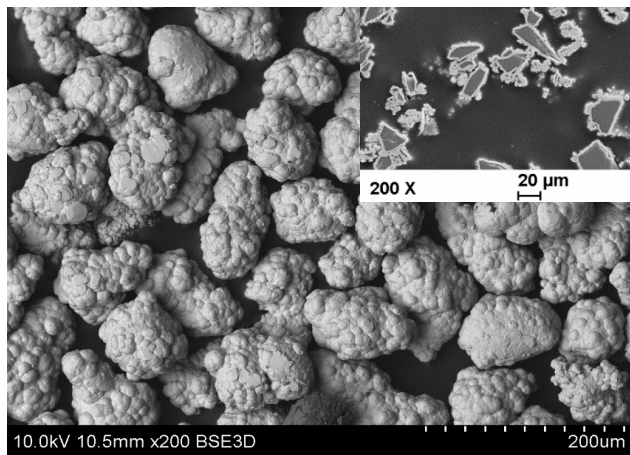


Fig. 2

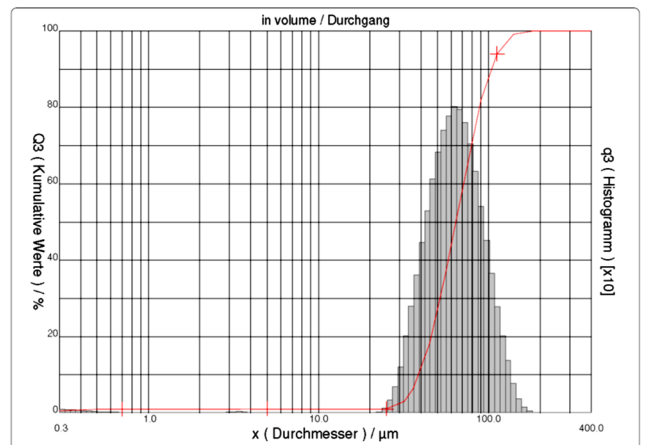
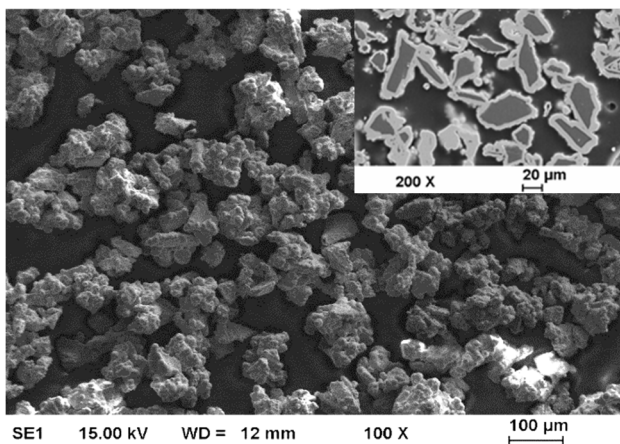


Fig. 3

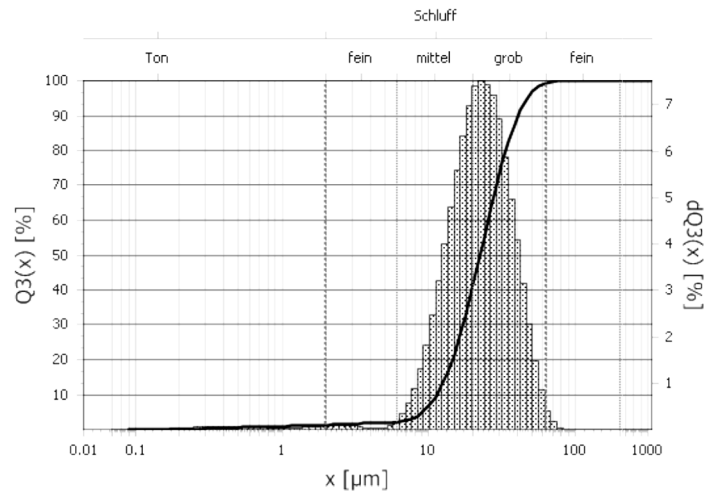
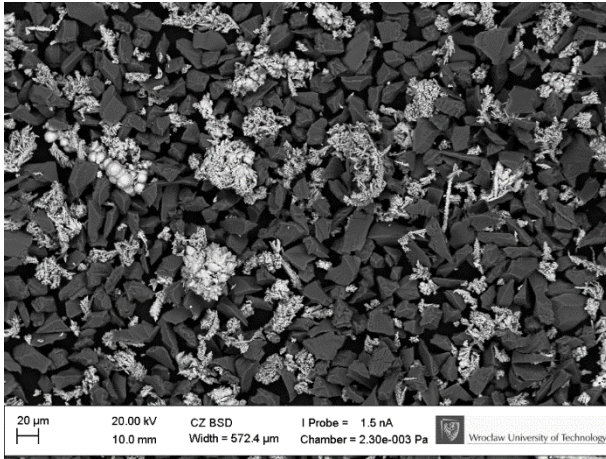
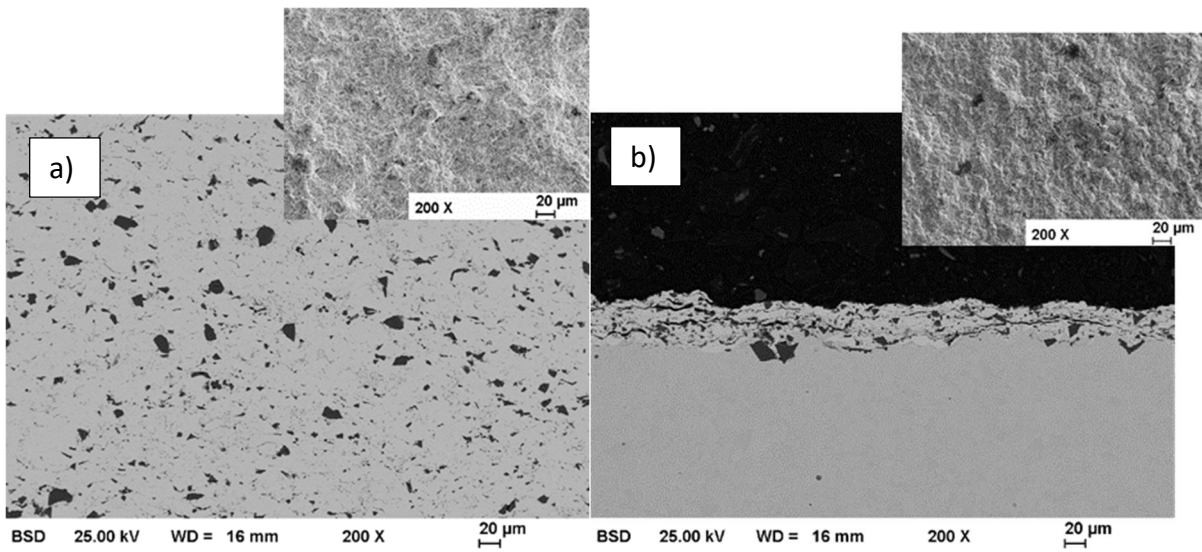


Fig. 4



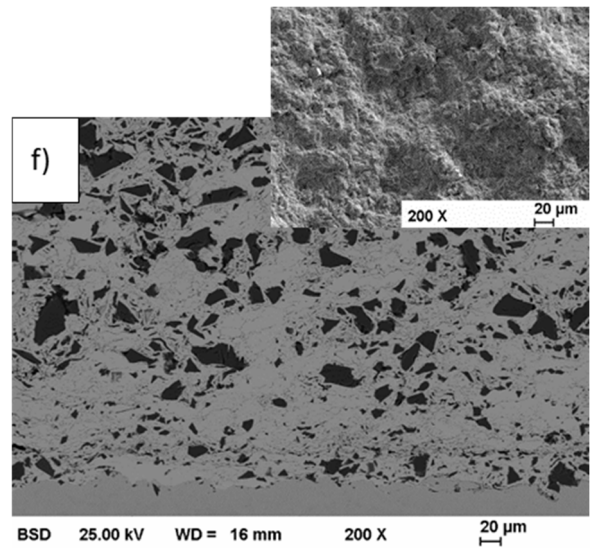
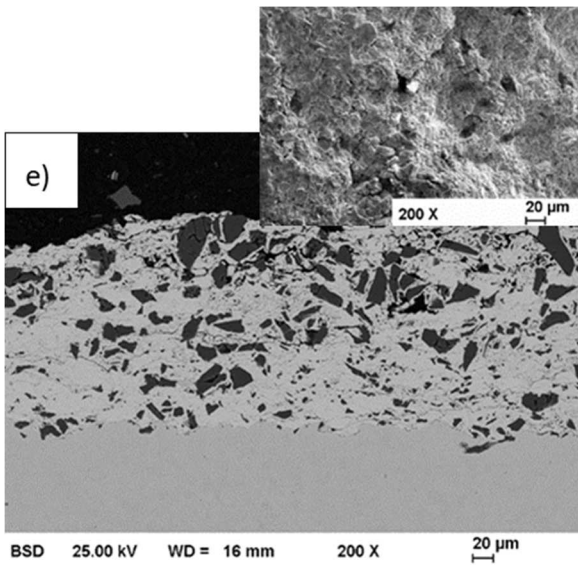
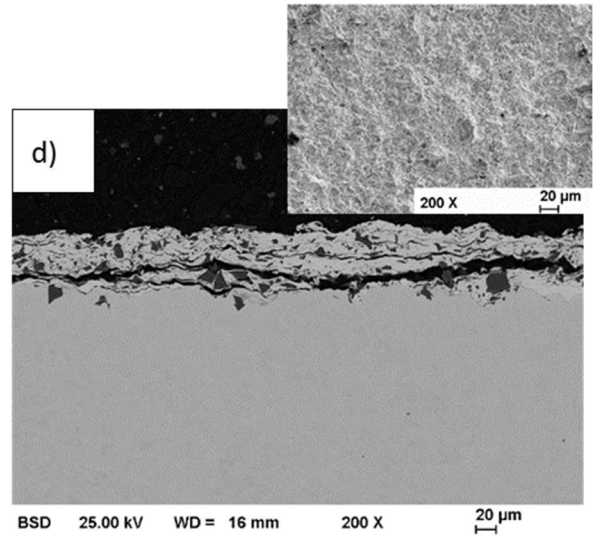
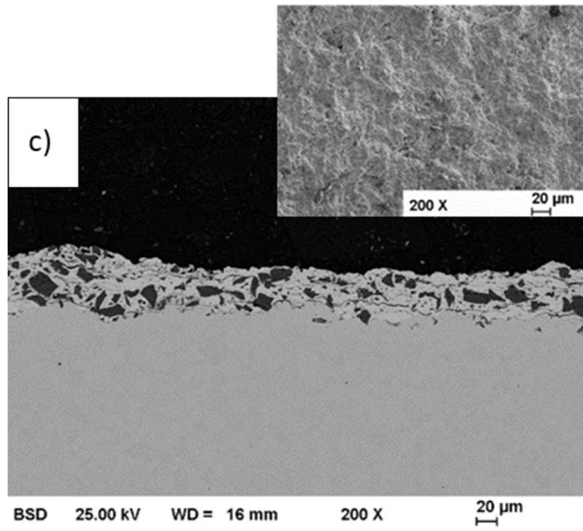


Fig. 5

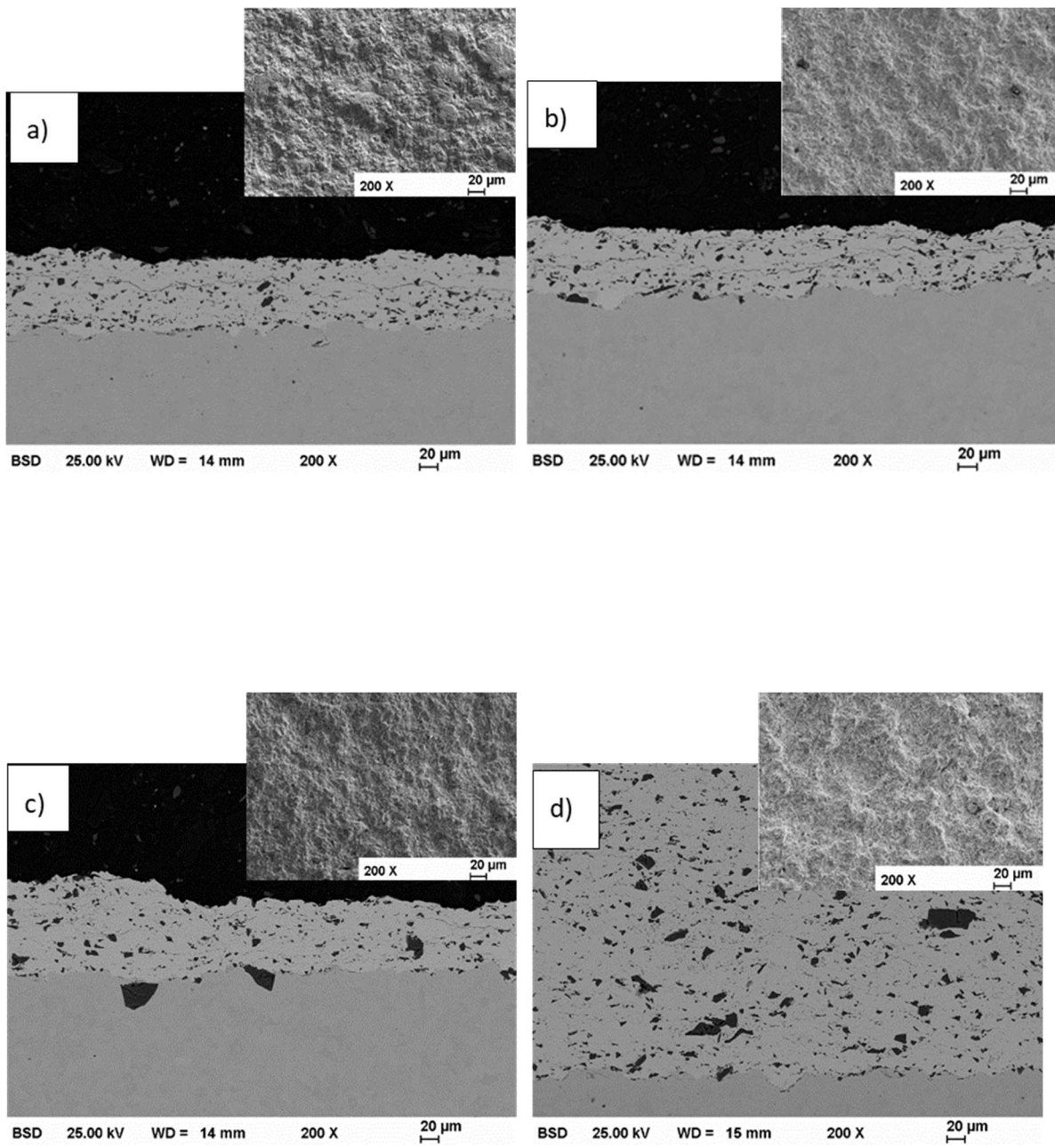


Fig. 6.

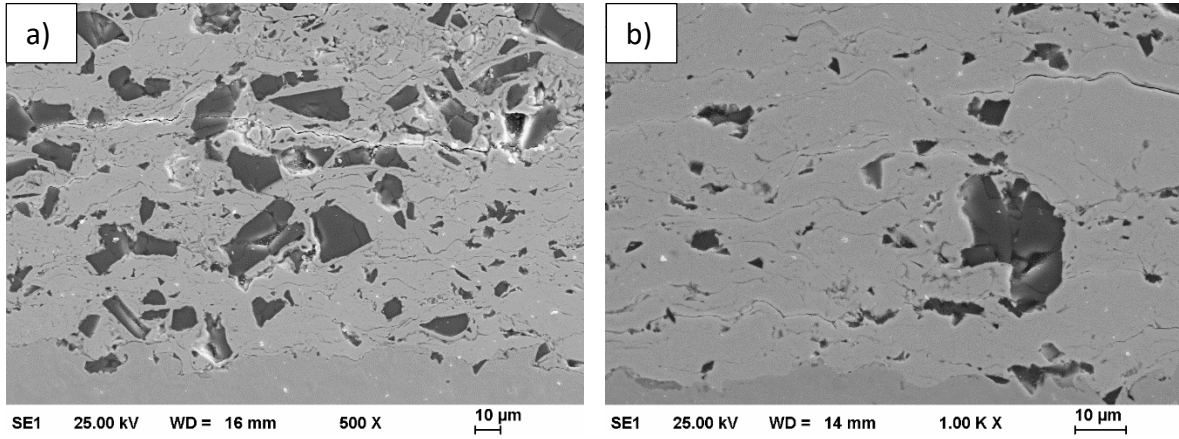


Fig. 7.

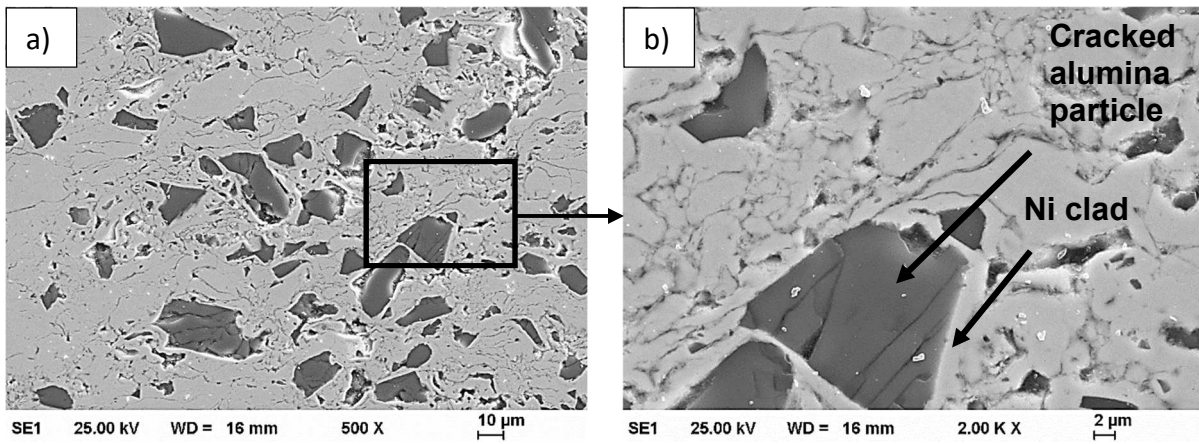


Fig. 8.

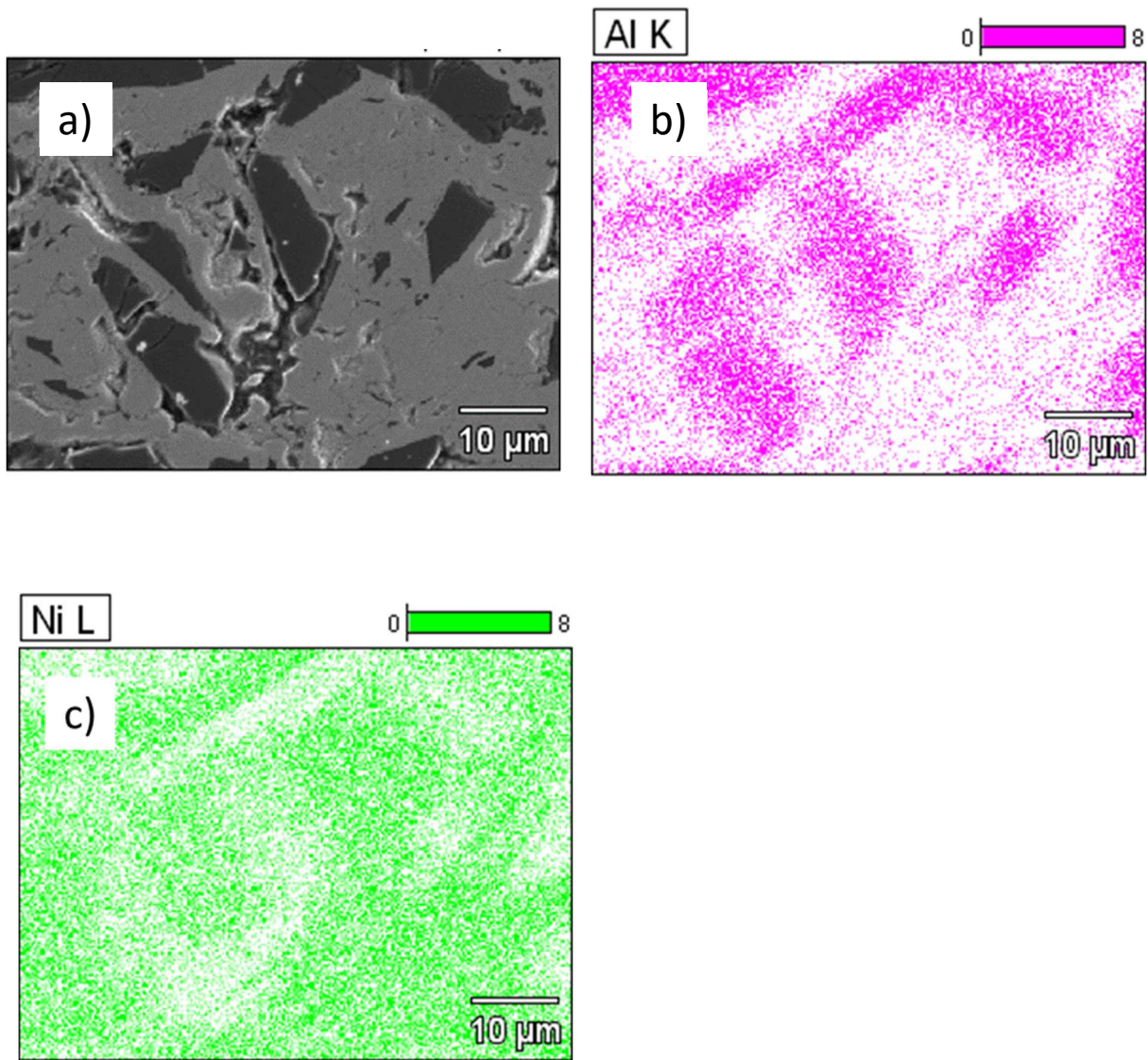


Fig. 9

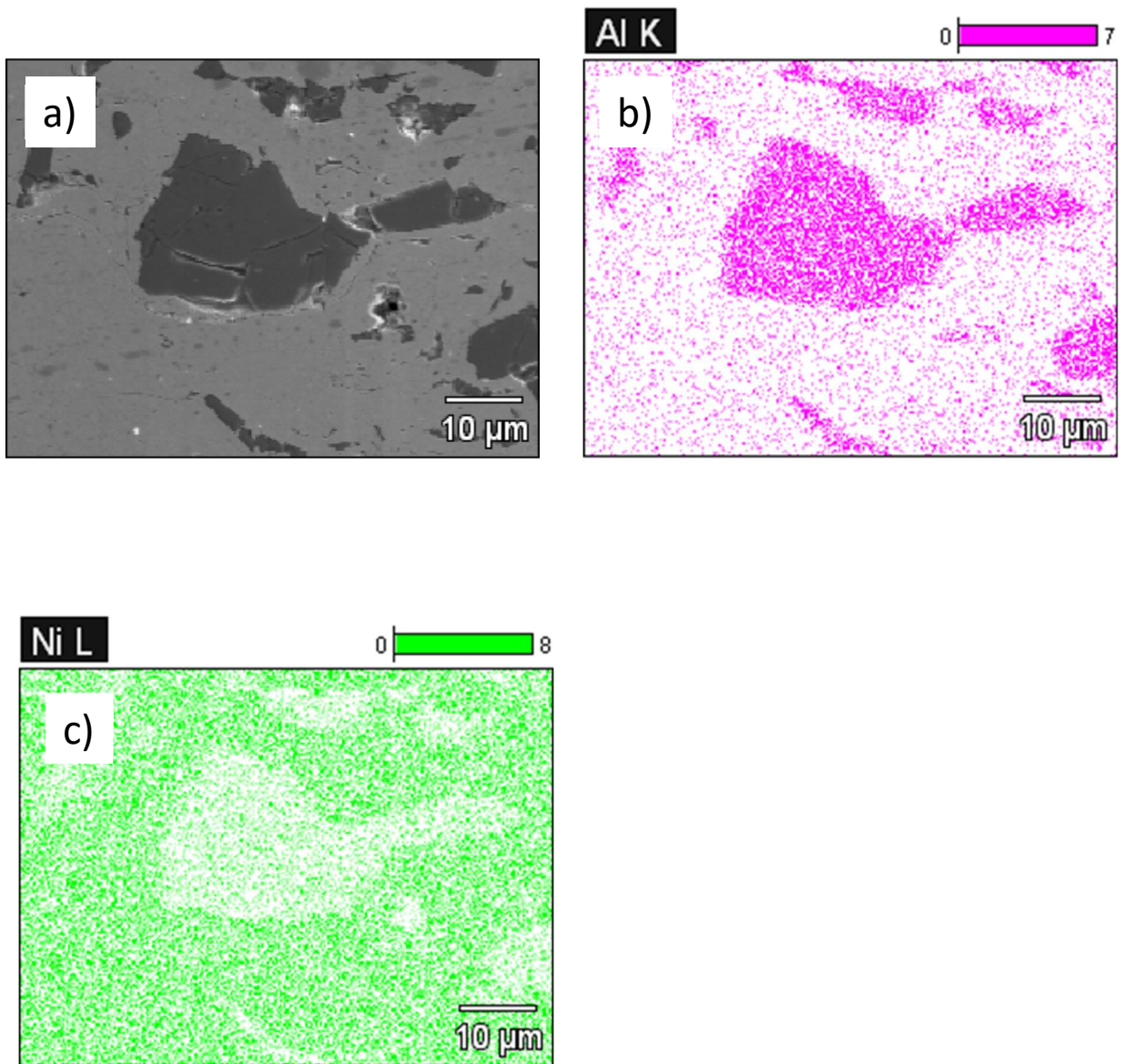


Fig. 10

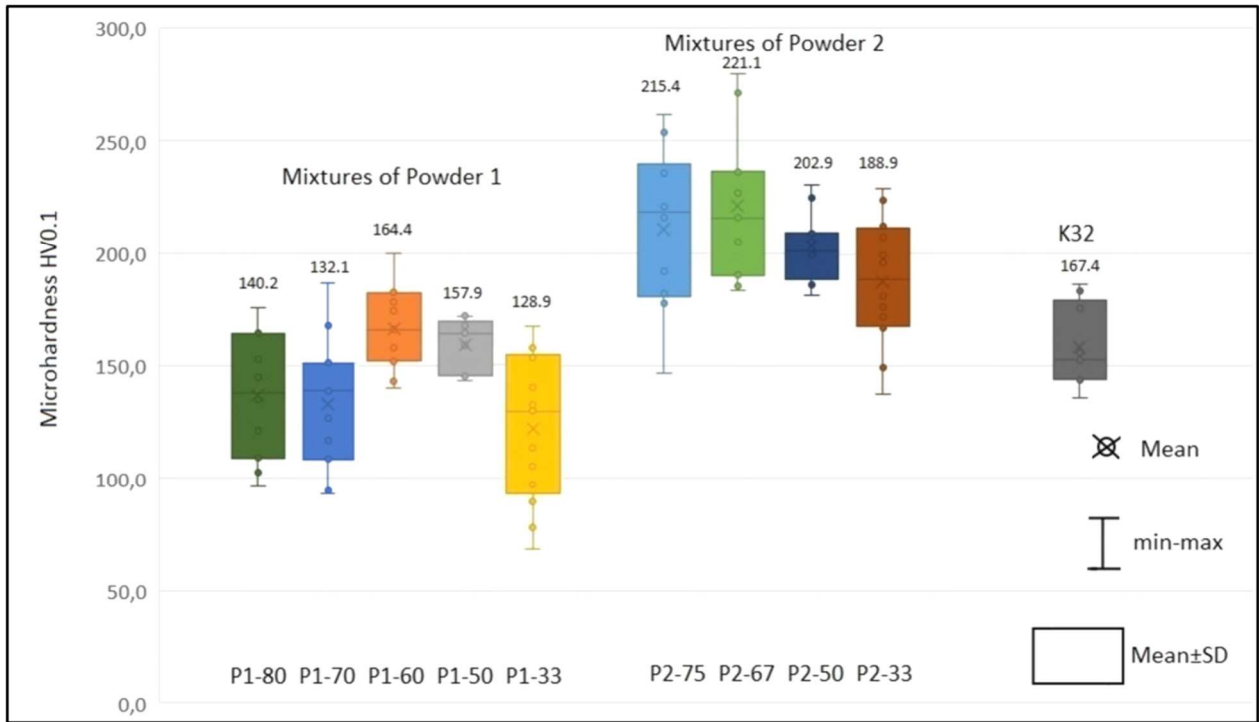


Fig. 11

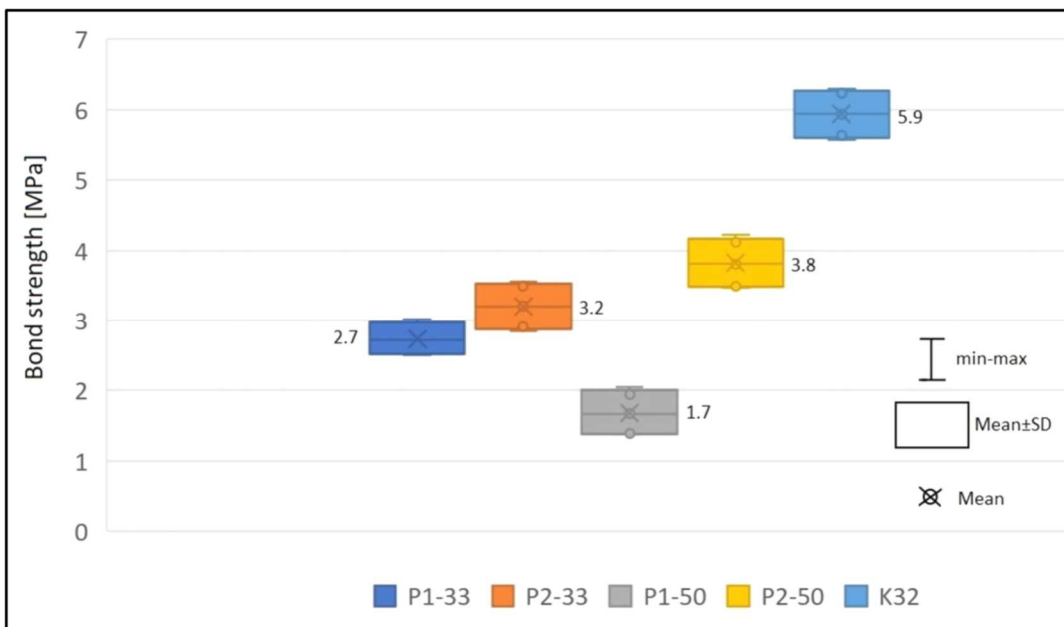


Fig. 12

## Tables

Table 1. Powders used to LPCS coatings deposition

Powder symbol	Powders used	Content of powders in mixtures, wt. %	
		Cladded powder	Commercial K32 powder
K32	K32	0	100
P1-80	Cladded powder # 1 and K32	80	20
P1-70		70	30
P1-60		60	40
P1-50		50	50
P1-33		33	67
P2-75	Cladded powder # 2 and K32	75	25
P2-67		67	33
P2-50		50	50
P2-33		33	67

Table 2. Results of graphical estimation of Al<sub>2</sub>O<sub>3</sub> content in the sprayed coatings and of their thickness reached during constant deposition time.

Coating sprayed using powder	The content of Al <sub>2</sub> O <sub>3</sub> in sprayed coating in wt. %		Coating thickness	
	Mean	Standard deviation	min	max
K32	7.3	0.2	680	850
P1-80	21.5	0.7	20	40
P1-70	30.5	1.1	40	80
P1-60	22.0	0.4	40	80
P1-50	24.6	0.9	160	190
P1-33	21.0	0.3	540	680
P2-75	9.8	0.1	75	100
P2-67	12.7	0.2	60	80
P2-50	9.3	0.2	90	120
P2-33	9.9	0.1	400	470